POLITECNICO DI TORINO
Repository ISTITUZIONALE

VNA-Based Skin Cancer Detection in the 500–750 GHz Frequency Range

Original
VNA-Based Skin Cancer Detection in the 500–750 GHz Frequency Range / Moda, S., Paonessa, F., Tobon Vasquez, J.A., Virone, G., Vipiana, F.. - ELETTRONICO. - (2026). (2026 IEEE International Symposium on Antennas and Propagation and USNC-URSI Radio Science Meeting Detroit (USA) 12-17 July 2026).

Availability:
This version is available at: 11583/3014930 since: 2026-08-28T08:39:58Z

Publisher:
IEEE

Published
DOI:

Terms of use:

This article is made available under terms and conditions as specified in the corresponding bibliographic description in the repository

Publisher copyright
IEEE postprint/Author's Accepted Manuscript

©2026 IEEE. Personal use of this material is permitted. Permission from IEEE must be obtained for all other uses, in any current or future media, including reprinting/republishing this material for advertising or promotional purposes, creating new collecting works, for resale or lists, or reuse of any copyrighted component of this work in other works.

(Article begins on next page)

08 November 2026

VNA-Based Skin Cancer Detection in the 500–750 GHz Frequency Range

S. Moda[(1)], F. Paonessa[(2)], J. A. Tobon Vasquez[(1)], G. Virone[(2)], and F. Vipiana[(1)]

[(1)] Dept. Electronics and Telecommunications, Politecnico di Torino, Torino, Italy
[(2)] Inst. of Electronics, Computer and Telecommunication Engineering (IEIIT), Consiglio Nazionale delle Ricerche (CNR), Torino, Italy

***Abstract*—Sub-terahertz waves are highly sensitive to tissue hydration levels, making them a promising non-invasive tool for skin cancer detection. This work validates the capabilities of a compact, contactless continuous-wave system to discriminate a synthetic lesion from surrounding tissue using a dedicated skin phantom. Depth-resolved reflectivity profiles and B-scan imaging demonstrate that the system can clearly resolve the lesion, highlighting its potential for dermatological applications.**

I. Introduction

Skin cancer is the most prevalent cancer worldwide and includes malignant neoplasms such as melanoma, which has the highest mortality rate, as well as non-melanoma skin cancers, including basal cell carcinoma (BCC) and squamous cell carcinoma (SCC), with approximately 5.4 million cases diagnosed annually in the United States alone [1].

Consequently, to mitigate the disease burden, accurate diagnosis and timely, effective treatment are essential; to this end, numerous electromagnetic-based technologies have been developed to support clinical management by addressing the invasiveness and long diagnostic delays associated with biopsy followed by histopathological examination, which remains the current gold standard for diagnosis. This can be attributed to the fact that alternative non-invasive techniques still exhibit several limitations, including limited penetration depth, bulky systems, the requirement for trained personnel, and often rely on contact-based probes, which introduce additional challenges [2].

Terahertz (THz) waves, owing to their non-ionizing nature and high sensitivity to tissue hydration levels, exhibit significant potential for skin cancer sensing and detection, offering a favorable trade-off between spatial resolution and penetration depth compared to microwave- and infrared-based techniques. This is because tumors, characterized by increased vascularization and consequently higher blood content than the surrounding healthy tissue, provide an endogenous contrast source for THz waves.

In this work, a compact, contactless continuous-wave (CW) sub-THz system operating in the WR-1.5 band (500-750 GHz) is presented for skin cancer applications, and preliminary measurements are performed on a dedicated phantom mimicking a BCC pattern surrounded by healthy skin (HS). This paper is based on the numerical analysis presented in [3].

II. Skin Phantom

Tissue-mimicking phantoms are essential for the development and validation of biomedical devices. By replicating the dielectric properties of biological tissues across the frequency bands of interest, they serve as reliable surrogates for real tissues, enabling controlled and repeatable measurements while addressing ethical constraints in experimentation.

The phantom used in this study is designed by taking as reference the complex permittivity ($\tilde{\varepsilon}$) measurements of HS and BCC reported by Nourinovin *et al.* in [4].

To quantify the dielectric contrast between pathological and healthy tissue, the following definition is adopted:

$$C(f) = \left| \frac{\tilde{\varepsilon}_{bg} - \tilde{\varepsilon}_{tg}}{\tilde{\varepsilon}_{bg}} \right|, \tag{1}$$

where $\tilde{\varepsilon}_{bg}$ and $\tilde{\varepsilon}_{tg}$ correspond to the frequency-dependent complex permittivity of the background tissue (HS) and the lesion target (BCC), respectively.

The skin phantom is therefore realized using mixtures of silicone rubber loaded with graphite powder and dielectrically characterized at 625 GHz through a fitting-based methodology applied to measurements performed with a contact truncated waveguide system under pressure monitoring. Table I shows that the contrast at 625 GHz between silicone rubber loaded with 5% graphite (SR5%) and pure silicone rubber (SR0%) is consistent with the contrast observed between BCC and HS in literature.

TABLE I
Dielectric contrast values at 625 GHz for different target–background pairs.

Target–background	C(625 GHz)
BCC-HS *max*	0.761
BCC-HS *min*	0.357
BCC-HS *average*	0.513
SR5%-SR0%	0.512

III. Measurement System

The compact probe, shown in Fig. 1, employs a WR-1.5 diagonal horn antenna to perform contactless reflectivity measurements on the skin or phantom under test. The horn, with a nominal gain of 26 dBi and a half-power beamwidth of $\sim 10°$, is mounted on a VDI WM-380 VNAX frequency extension module in a downward-facing monostatic configuration and held vertically by a support stand.

The module connects to a Rohde & Schwarz ZNA67 Vector Network Analyzer (VNA), with the phantom positioned circa 13 mm below the horn. A motorized linear translation stage,

equipped with a laboratory elevation jack as sample holder, provides 6 μm positioning repeatability over a travel range of 300 mm. During each session, the stage moves along a 20 mm scan line with 300 μm steps while the VNA measures reflection coefficients (S_{11}) by performing frequency sweeps across 500–750 GHz. Software sweep triggering ensures synchronization between stage position and measurements.

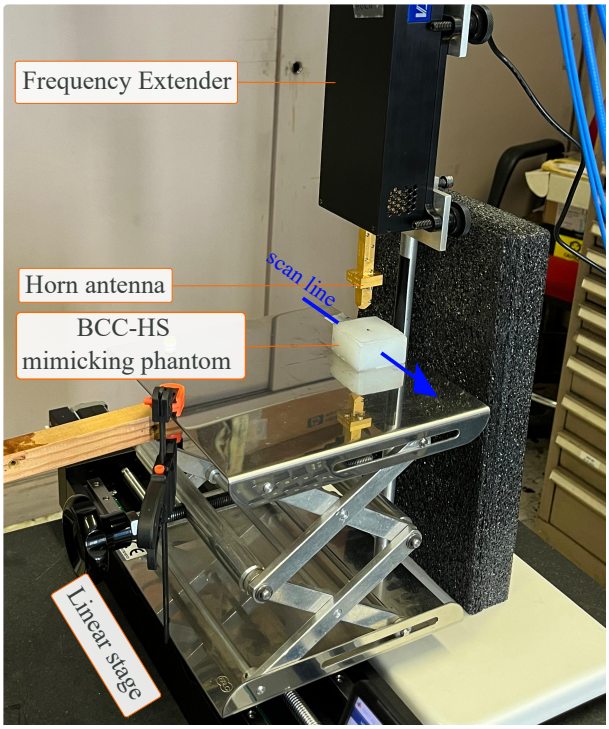

Fig. 1. Measurement setup close-up showing the compact probe mounted vertically on a metal stand, with the phantom supported by an elevation jack and positioned on a high-precision linear stage.

Each S_{11} trace includes 1001 frequency points, corresponding to a maximum unambiguous range of approximately 600 mm. The total scan duration is on the order of 5 minutes.

A single-port offset–short–matched-load (OSM) calibration is performed at the extender flange prior to measurements to define a consistent reference plane for the reflectivity analysis presented in Sect. IV.

’

IV. Results and Discussion

The capability to discriminate the presence of a BCC lesion from the surrounding healthy skin is evaluated by deriving spatially resolved reflectivity profiles from the measured S_{11} data. A time-domain analysis based on the inverse fast Fourier transform (IFFT) is then performed to convert the frequency-domain measurements into the spatial domain, revealing the backscattered response as a function of penetration depth [5].

From the reflectivity profiles, peaks associated with the air–sample interface can be clearly identified. The locally varying amplitudes observed at this interface arise from spatial variations in dielectric contrast along the linear scan in the vicinity of the target.

Depth-resolved reflectivity profiles are arranged along the scan line and mapped to a colormap, producing a B-scan where columns represent local profiles and color encodes signal intensity across position and depth. Figure 2 shows a representative image generated by scanning a phantom featuring a surface BCC-like pattern, realized by regions of SR5% with a thickness below 1 mm embedded in an SR0% background. The corresponding scan line is also highlighted.

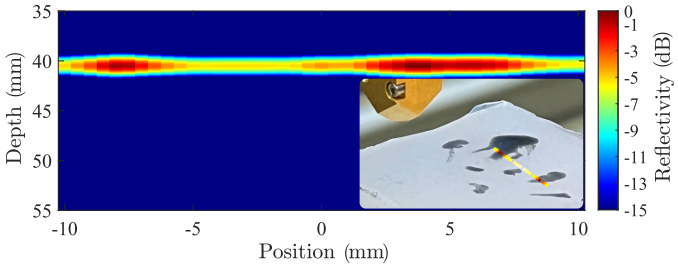

Fig. 2. B-scan image of a silicone rubber phantom featuring a BCC target pattern mimicking a skin lesion surrounded by healthy skin, acquired in the WR-1.5 frequency band.

The resulting image clearly resolves the targets at their correct locations, demonstrating the capability to accurately differentiate a potential BCC lesion from the surrounding HS and further highlighting the potential of sub-THz waves for dermatological applications, with the system presented here featuring a compact, contactless design operating in the WR-1.5 frequency band.

ACKNOWLEDGEMENT

This work has been supported in part by the PNRR-NGEU project, funded by the Ministry of University and Research (MUR, DM118/2023).

References

[1] American Cancer Society. *Cancer Statistics* [Online]. Available: https://www.cancer.org/cancer/types/basal-and-squamous-cell-skin-cancer/about/key-statistics.html. Accessed: Jan. 23, 2026.

[2] S. A. R. Naqvi, I. Jiji Rajmohan, F. Xue, D. Foong, and A. Abbosh, “Electromagnetic Techniques and Systems for Noninvasive Skin Cancer Detection and Classification: Current Status and Future Perspectives,” *IEEE Transactions on Instrumentation and Measurement*, vol. 74, pp. 1–24, 2025.

[3] S. Moda, J. A. Tobon Vasquez, G. Virone, and F. Vipiana, “Dielectric Contrast Assessment for Skin Cancer Detection in the Terahertz Band,” in *2025 IEEE International Symposium on Antennas and Propagation and North American Radio Science Meeting (AP-S/CNC-USNC-URSI)*. IEEE, 2025, pp. 313–315.

[4] S. Nourinovin, M. M. Rahman, S. J. Park, H. Hamid, M. P. Philpott, and A. Alomainy, “Terahertz dielectric characterization of three-dimensional organotypic treated basal cell carcinoma and corresponding double Debye model,” *IEEE Transactions on Terahertz Science and Technology*, vol. 13, no. 3, pp. 246–253, 2023.

[5] Rohde & Schwarz, “Time Domain Measurements using Vector Network Analyzer ZNA,” Available: https://scdn.rohde-schwarz.com/ur/pws/dl_downloads/dl_application/application_notes/1ep83/1EP83_0e_TimeDomain_ZNA7.pdf, 2020, Accessed: Jan. 23, 2026.